New Approach to Short-Range Ordering in GP(2) Zones in Al-3.82wt. %Cu Alloy

Moritaka HIDA**, Nobuo MATSUMORI* and Hikaru TERAUCHI*

Synopsis

X-ray diffuse scatteing intensity measurement has been carried out for the Al-3.82%Cu single crystal in which GP(2) zones are found. The two dimensional equi-intensity contour maps in $h_1 h_2 0$ plane are obtained from surveying around several reflections. The diffuse intensity around 2 1 0 reflection, which shows a cross like streak, is carefully examined. Warren-Cowley short-range order parameters, α_i, are estimated from the diffuse intensities around 2 1 0 reflection. The component of the intensities coming from atomic dis-placements was subtracted from the total diffuse inten-sity. It is found that the equi-intensity contours after the correction of the atomic displacements shows an anisotropic distribution and the GP(2) zone is an ellipsoid with a modified layer structure.

1. Introduction

There have been many investigations on GP(2) zones in Al-Cu alloy. The first investigation was carried out by Guinier [1], and he has proposed the model of the zones which are constructed of the ordered four layers' structure made of aluminium atomic layer and three copper rich layers[one of them seems to be 100at.%Cu, the others 20 to 25at. %Cu]. Gerold[2] and Baur[3] have reported another model consisting of

---

* Department of Physics, Kwansei Gakuin University, Nishinomiya 662, Japan
** School of Engineering, Okayama University, Okayama 700, Japan.

pure aluminium and pure copper layers to explain the X-ray diffuse in-
tensity. By the observation of the diffraction contrast in electron
micrographs of thin foil of Al-Cu alloy, Nicholson and Nutting [4]
showed that the matrix lattice surrounding GP(2) zone is deformed.
The layer structures of GP(2) zones has been also investigated using
the two-beam lattice fringe technique [5, 6] and the weak-beam technique
[7] of electron microscopy.

In this paper, the precise measurements of the x-ray diffuse scat-
tering from GP(2) zones are presented to elucidate the short-range
ordering of copper atoms in the zones. For this purpose, an atomic
size effect in the X-ray diffuse intensity distribution around some
symmetrical points in the reciprocal space has been considered by
employing the same formula as those in Sparks [8] and Borie's [8,9]
method of calculating short-range order parameters, α_i.

2.   Short-range Ordering and X-ray Diffuse Scattering

The coherently scattered intensity from a binary alloy can be writ-
ten as the sum of the intensity associated with the fundamental Bragg
peaks, I_F, and the total diffuse intensity, I_D, where I_D can be written
as the sum of three terms

$$I_D = N\ x_A\ x_B(f_A - f_B)^2(I_{SRO} + I_{SE} + I_{TDS.H}). \quad \cdots\cdots\cdots\cdots (1)$$

Where I_{SRO} is the scattering due to local order, I_{SE} is the so-called
size-effect term and $I_{TDS.H}$ is due to first order thermal diffuse and
Huang scattering. N is the number of atoms in X-ray irradiation, x_A
and x_B the atomic fractions of components A and B, respectively, and
f_A and f_B their atomic scattering factors. Each term can be expanded
to a trigonometric series in electron unit.

$$I_{SRO} = \underset{lmn}{\Sigma\Sigma\Sigma}\ \alpha_{lmn}\ \cos 2\pi\ (h_1 l + h_2 m + h_3 n) \cdots\cdots\cdots\cdots\cdots (2)$$

$$I_{SE} = -\underset{lmn}{\Sigma\Sigma\Sigma}(h_1\gamma^x_{lmn} + h_2\gamma^y_{lmn} + h_3\gamma^z_{lmn})\ \sin 2\pi(h_1 l + h_2 m$$

$$+ h_3 n) \cdots\cdots\cdots\cdots\cdots\cdots\cdots\cdots\cdots\cdots\cdots (3)$$

$$I_{TDS.H} = \Sigma\Sigma\Sigma(h_1^2\delta_{1mn}^x + h_2^2\delta_{1mn}^y + h_3^2\delta_{1mn}^z + h_1h_2\varepsilon_{1mn}^{xy}$$

$$+ h_2h_3\varepsilon_{1mn}^{yz} + h_3h_1\varepsilon_{1mn}^{zx})\cos2\pi(h_1l + h_2m + h_3n)\ldots.(4)$$

The integers 1,m,n define a particular lattice site according to the relation in f.c.c. lattice

$$\gamma_{1mn} = 1a_1/2 + ma_2/2 + na_3/2$$

where a_1,a_2,a_3 are the translational vectors of the cubic unit cell, and h_1,h_2,h_3 are the continuous coordinates in reciprocal space. The α_{1mn} (or α_i) are the short-range order parameters defined by

$$\alpha_{1mn} = 1- p_{1mn}^{AB}/x_B$$

where p_{1mn}^{AB} (or p_i^{AB}) is the probability of finding a B atom at the end of a vector γ_{1mn} (or r_i, radius ith shell) when the origin is occupied by an A atom. Other Fourier coefficients are given by

$$\gamma_{1mn}^x = 2\pi[F_{AA}\langle X_{1mn}^{AA}\rangle + F_{AB}\langle X_{1mn}^{AB}\rangle + F_{BB}\langle X_{1mn}^{BB}\rangle]$$

$$\delta_{1mn}^x = -2\pi^2[F_{AA}\langle(X_{1mn}^{AA})^2\rangle + F_{AB}\langle(X_{1mn}^{AB})^2\rangle + F_{BB}\langle(X_{1mn}^{BB})^2\rangle]$$

$$\varepsilon_{1mn}^{XY} = -4\pi^2[F_{AA}\langle X_{1mn}^{AA}\rangle + F_{AB}\langle X_{1mn}^{AB}Y_{1mn}^{AB}\rangle + F_{BB}\langle X_{1mn}^{BB}Y_{1mn}^{BB}\rangle]$$

where

$$F_{AA} = f_A^2[(x_A / x_B) + \alpha_{1mn}] / (f_A - f_B)^2$$

$$F_{AB} = 2f_Af_B(1 - \alpha_{1mn}) / (f_A - f_B)^2$$

$$F_{BB} = f_B^2[(x_B /x_A) + \alpha_{1mn}] / (f_A - f_B)^2$$

The definition of γ_{1mn}^y, γ_{1mn}^z, δ_{1mn}^y, δ_{1mn}^z, ε_{1mn}^{yz} and ε_{1mn}^{zy} are also analogous to the above mentioned Fourier coefficients. X_{1mn}^{ij}, Y_{1mn}^{ij} and Z_{1mn}^{ij} are the deviations of an i atom and a j atom from their average positions. The averages $\langle X_{1mn}^{AA}\rangle$, etc. are taken for all i-j pairs separated by constant distnce ($\overline{r_{1mn}^i}$ - $\overline{r_{1mn}^j}$).

It has been considered by Sparks [9] et al. that the term (4) has

little effects on α_{1mn} at the reciprocal points far away from the Bragg reflections.

3. Experimental Procedure

A conventional double axes X-ray spectrometer was used during this work. As the X-ray source $MoK\alpha_1$ radiation monocromatized by a flat plate of LiF single crystal was employed. $MoK\alpha_2$ component in $MoK\alpha$ radiation was cut off by knife edges of a divergent slit with 0.15 mm in width and 4 mm in hight placed at a distance 50 mm from the mono-chromator. Scattered beam from a sample impinges into a scintillation counter through two slits with 0.3 mm and 1mm in width respectively. The horizontal and vertical angular resolutions were estimated as 0.09° and 2.5° respectively. The received X-ray was counted through a single channel pulse height analyser to eliminate the components of $\lambda/2$ and $\lambda/3$. The intensity due to the harmonics could not be observed in the intensity profile around 1 0 0 reflection of Al-3.82wt.%Cu solid solu-tion single crystal. The intensity measurement was carried out at 295 K. The stability of the X-ray source and of the counting electronics was checked many times by detecting the 1 0 0 diffuse scattering in-tensity during the measurement process.

99.996% purity aluminium and 99.996% copper were melted in a high purity Alumina crucible in atmosphere. After the ingot of 15 mm$^\phi$ X 80 mm was hot-forged to 2 mm in thickness, the strip was cold-rolled to 0.6 mm in thickness. The single crystals were produced by the same strain annealing method as that of Hida et al [10]. The dimensions of the single crystal used for X-ray scattering intensity measurement were 5 mm in width, 0.6 mm in thickness and 12 mm in length. This crystal was homogenized at 775K and then quenched into iced water. After age-ing of an hour at 353K and 24 hours at 433K, GP(2) zones were nucleated The resistivity changes (see fig.1, curve A) are recognized as the for-mation of GP(2) zones [10, 11].

4. Results and Anlyses

Figure 2 shows the observed equi-intensity contour map of diffuse scattering around 2 1 0 reciprocal point. The vectors q// and q⊥ in the figure are the wave vector parallel and perpendicular to the re-
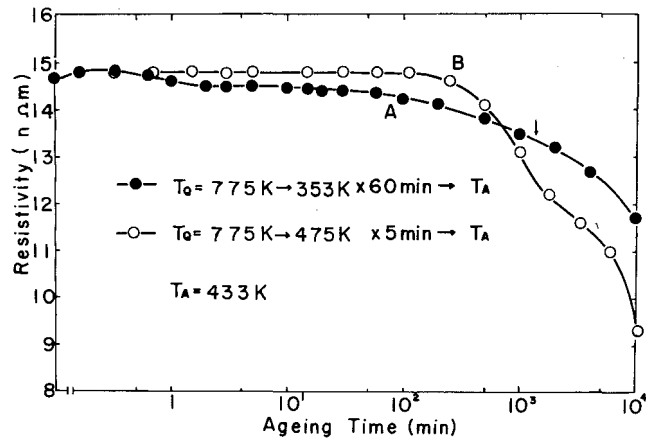
Fig. 1 Changes of electrical resistivity during ageing at
433K in Al-3.82wt.%Cu alloy quenched from 775K.
The intermediate heat treatment is 353K x 60 min. and
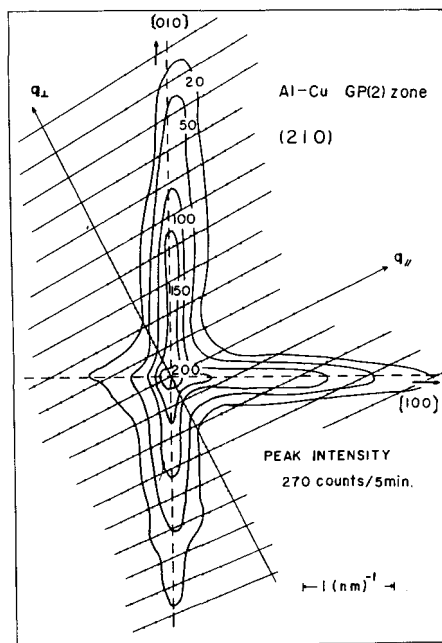475K x 5 min. for curve A and B respectively.

Fig. 2 The diffuse scattering distribution from GP(2) zones,
looking around (2 1 0) reflection in the h_1 h_2 0
plane. The black dots in the figure present the
measurement points.

ciprocal lattice vector G = $2a_1^* + a_2^*$.

    The each black dot in the figure means the point, where the inten-
sity was measured for 5 minutes at 295K. Two diffuse streaks belonging
to [1 0 0] and [0 1 0] directions were detected. The asymmetric
feature can be considered to depend on the size effect of the equation
(3) in section 2. The diffuse intensities, caused by GP(2), around
1/2 0 0, 1 0 0, 1 1 0, 2 0 0 and 2 2 0 reflections were also measured.
The equi-intensity contours of 100 counts per 5 minutes are shown in
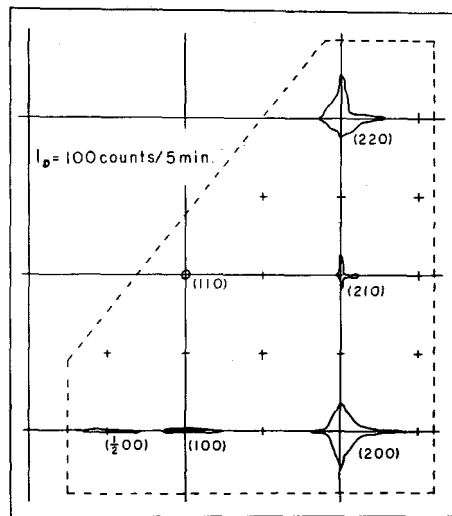fig.3.

Fig. 3 The equi-intensity (100 counts per 5 minutes) countors
        in h_1 h_2 0 plane.

    The equation of diffuse intensity for f.c.c. crystal was written,
provided $I_{TDS.H}$ is neglected as mentioned in section 2, as follows.

$$I_D = I_{SRO} + I_{SE} = \sum_{lmn}\sum\sum \alpha_{lmn}\cos 2\pi(h_1 l + h_2 m + h_3 n)$$

$$-\sum_{lmn}\sum\sum(h_1\gamma_{lmn}^x + h_2\gamma_{lmn}^y + h_3\gamma_{lmn}^z)\sin 2\pi(h_1 l$$

$$+ h_2 m + h_3 n)\ldots\ldots\ldots\ldots\ldots\ldots\ldots(5)$$

As it can be considered that all of α_{lmn} which belong to the ith near-
est neighbour atoms are equivalent, that is to say, $\alpha_{lmn} = \alpha_{mnl} = \alpha_{nlm}$

$= \alpha_{\overline{1}\overline{m}\overline{n}} = \alpha_{\overline{1}mn} = \alpha_{\overline{1}\overline{m}n}$ etc., the first term is written as follows.

$$I_{SRO} = \sum_i z_i \alpha_i C_i (h_1 \ h_2 \ h_3)$$

where z_i is the coordinate number of the ith shell, for example, $z_1 =$ 12 for the f.c.c. lattice, C_i is the sum of cosine terms. The measure-ment of intensity have been carried out in the reciprocal $h_1 \ h_2 \ 0$ plane, and then the term I_{SRO} is consequently expressed as follows

$$
\begin{aligned}
I_{SRO} =\ & \alpha_0 + 12\alpha_1 [(\cos\pi h_1 \cos\pi h_2 + \cos\pi h_1 + \cos\pi h_2)/3] \\
& + 6\alpha_2 [(\cos 2\pi h_1 + \cos 2\pi h_2 + 1)/3] \\
& + 24\alpha_3 [(\cos 2\pi h_1 \cos\pi h_2 + \cos\pi h_1 \cos\pi h_2 \\
& \qquad + \cos\pi h_1 \cos\pi h_2)/3] \\
& + 12\alpha_4 [(\cos 2\pi h_1 \cos 2\pi h_2 + \cos 2\pi h_1 + \cos 2\pi h_2)/3] \\
& + 24\alpha_5 [(\cos 3\pi h_1 \cos\pi h_2 + \cos\pi h_1 \cos 3\pi h_2 + \cos 3\pi h_1 \\
& \qquad + \cos 3\pi h_2 + \cos\pi h_1 + \cos\pi h_2)/6] \\
& + 8\alpha_6 [\cos 2\pi h_1 \cos 2\pi h_2] \\
& + 48\alpha_7 [(\cos 3\pi h_1 \cos 2\pi h_2 + \cos\pi h_1 \cos 3\pi h_2 \\
& \qquad + \cos 2\pi h_1 \cos\pi h_2 + \cos 3\pi h_1 \cos\pi h_2 \\
& \qquad + \cos 2\pi h_1 \cos 3\pi h_2 + \cos\pi h_1 \cos 2\pi h_2)/6] \\
& + 6\alpha_8 [(\cos 4\pi h_1 \cos 4\pi h_2 + 1)/3] \\
& + \quad ------ \quad \dots\dots\dots\dots\dots\dots\dots\dots\dots(5a)
\end{aligned}
$$

The second term I_{SE} is expanded to series of sine, provided that the symmetry of tetragonality of GP(2) zones are considered, i.e. $\gamma^x_{1mn} = -\gamma^x_{\overline{1}\overline{m}\overline{n}}$, $\gamma^x_{11n} = \gamma^y_{11n} \neq \gamma^z_{11n}$, $\gamma^x_{0mn} = \gamma^y_{10n} = \gamma^z_{1m0} = 0$, as follows.

$$- I_{SE} = 2(h_1 + h_2)\gamma^x_{110}[\sin\pi(h_1 + h_2)] + 2(h_1 - h_2)\gamma^x_{1\bar{1}0}$$

$$x [\sin\pi(h_1 - h_2)] + 4h_1\gamma^x_{101}[\sin\pi h_1] + 4h_2\gamma^y_{011}[\sin\pi h_2]$$

$$+ 2h_1\gamma^x_{200}[\sin 2\pi h_1] + 2h_2\gamma^y_{020}[\sin 2\pi h_2] \quad \ldots\ldots\ldots\ldots\ldots(5b)$$

On calculating the parameters by using the least squares method, the intensity contour around 2 1 0 reflection is used, because the Bragg scattering is absent at 2 1 0 point and also the effect of thermal diffuse intensity is considered to be enough small at the comparatively low indices h_1 h_2 0 [12] . It is also assumed that Compton modified scattering is almost constant in the region where the measurement is carried out. The contribution of the diffuse scattering from the matrix was subtracted as a flat back ground around 2 1 0 reflection. It is assumed that there is almost no contribution of the matrix to the diffuse intensity used on calculating α_i.

The region where the intensity was measured around 2 1 0 reflection, $h_1 = 1.89 - 2.22$ and $h_2 = 0.87 - 1.16$, was divided into grids of $\Delta h_1 = \Delta h_2 = 0.01$ in width, and the region of $h_1 = 1.30 - 1.70$ and $h_2 = 0.30 - 0.70$ was divided into $\Delta h_1 = \Delta h_2 = 0.02$ in width. The intensities observed at 1420 points around 2 1 0 reflection employed as the I_D values, in equations (5a) and (5b).

The optmum α_1 to α_8 and γ_{lmn} are calculating by the least squares method with the computer FACOM 230-38. The α_0 must be determined experimentally by measuring the absolute intensity of diffuse scattering from zones as it had been obtained by Moss [13] for Cu_3Au alloy. But α_0 was normalized to be unity in the present work. The results obtained are tabulated in Table 1. It was found that there had been the stability of the solution in putting one to eight to the suffix i of α_i. Figure 4 shows the short-range order parameters for α_{lmn} on distance γ_{lmn}.

In order to synthesize the diffuse intensity in two-dimensional reciprocal space, the α_{lmn}, α_0 to α_8, obtained from the above mentioned method were put into the equation (5a). Figure 5 shows the diffuse intensity, where the size effects have been excluded. It is found that the equi-intensity contour has an anisotropy elongated to [1 0 0] direction around 1 0 0 reflection and to [0 1 0] direction around 2 1 0 reflection.

Table 1

The optimum α_{1mn} and γ_{1mn} calculated by the least squares method

neighbour	1 m n	α_{1mn}
1	1 1 0	0.023
2	2 0 0	-0.234
3	2 1 1	0.016
4	2 2 0	0.095
5	3 1 0	-0.030
6	2 2 2	-0.068
7	3 2 1	0.014
8	4 0 0	-0.048

$$\gamma^x_{110} = -0.229 \qquad \gamma^x_{1\bar{1}0} = -0.025$$

$$\gamma^x_{101} = 0.077 \qquad \gamma^x_{200} = -0.227$$

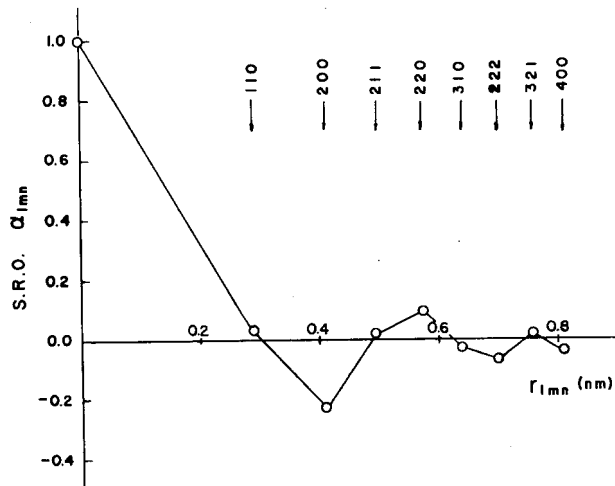$$\gamma^y_{011} = 0.403 \qquad \gamma^y_{020} = 0.117$$

Fig. 4 The short-range order parameters α_{1mn} as a function of r_{1mn}. α_0 is normalized to unity.
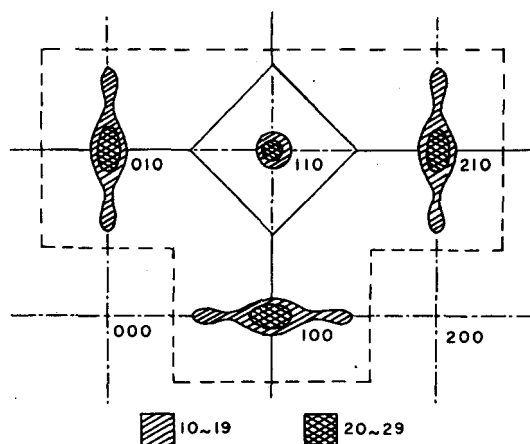
Fig. 5   The diffuse scattering distribution synthesized from
         the calculated values of α_{lmn} . The intensity con-
         tours satisfy the f.c.c. symmetry in the first Brillouin
         zone.

5. Discussion

    The determination of the short-range order parameters is an inter-
esting point of view in GP(2) zones. It is particularly important to
estimate the reasonable lattice distortion in GP(2) zone for obtaining
the short-range order parameters. In the first approximation, we took
the size effect up to the second nearest neighbours. And then we
prefered the tetragonal symmetry as the size effect of GP(2) zone to
the cubic symmetry, because the standard deviation of the least squares
method become small by adopting the tetragonal symmetry. The suitabil-
ity of this approximation must be reflected in the diffuse intensity
contour of fig. 5. It is important matter that the equi-intensity
contour for which the size effects have been excluded has an anisotropy
elongated to [0 1 0] direction around 2 1 0 reflection. After all,
the problem lies in the application of α_i which should be used for some
sort of spherical zone [14]. In the case which we, however, make bold
to apply the α_i to evern disk shaped GP(2) zones, characteristic of
fluctuation of solute concentration in GP(2) zone will be reflected in
atomic interaction or the correlation length which will be mentioned
later.

It is reasonable that a given fluctuation of copper concentration in GP(2) zones exists in the direction not only of parallel but also of perpendicular to the disk shaped zone, considering the dumping oscillation of α_{lmn} versus r_{lmn} as in figure 4. That is to say, the GP(2) zone's layer structure constructed of layers of copper and of aluminium atoms would not be always an appropriate model. If the correlation function is simply assumed as

$$\Phi(\gamma,\gamma') + (A \exp(-|\gamma - \gamma'|/\Lambda))/|\gamma - \gamma'|$$

where Λ is thecorrelation length, its Fourier transform gives the diffuse intensity as follows.

$$I_{SRO} = \Phi(q) = A / (\Lambda^{-2} + q^2)$$

This shows that the diffuse profile is regarded as Lorentzian. The correlation lengths of the solute concentration obtained grafically from the relation, the inverse of the synthesized intensity versus the scattering wave vector q squared, are nearly 4.8 nm in length and 10 nm in diameter respectively as shown in figure 6.
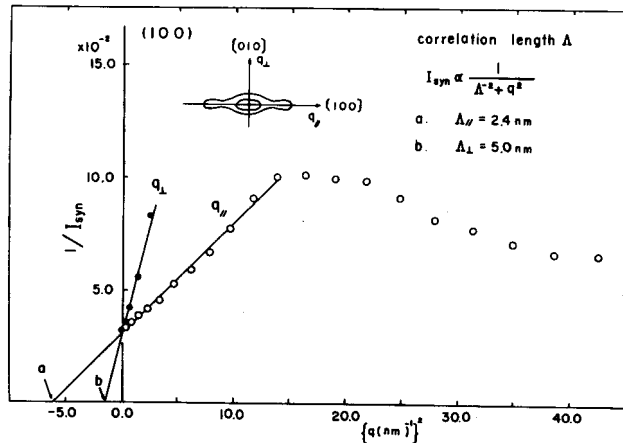

Fig. 6 The inverse of the synthesized diffuse intensity I_{syn} as a function of wave vector q squared. The correlation length of a given fluctuation of Cu solutes in GP(2) zones are obtained from this function.

The diffuse scattering intensity synthesized from the values of α_{lmn} shows an anisotropy which satisfies the f.c.c. symmetry (see figure 5). This implies that the short-range order interaction in the system is anisotropic and GP(2) zone is an ellipsoids, which is somewhat different from the layer structure. If α_i is connected to a given elastically atomic interaction not to the probability function, it seems to be reasonable that GP(2) zone has the f.c.c. symmetry and a given anisotropy of the ellipsoid. Such a quality has been found for a dielectrc, $NiCr_2O_4$ as an example [15].

Linear embryos of GP(2) zones may be formed in the matrix at the early stage of the phase transition. As the atomic interaction, however, occures among the embryos, some of them have a chance to nucleate an ellipsoid of GP(2) zone by the attractive force among the embryos. The ellipsoidal nucleus may be related to the correlation length, Λ corresponded to the phase of each zone. The stability of the nucleus of GP(2) zone will be discussed in terms of a phase motion partially reported by Frenkel et al [16]. and Horovitz et al [17].

6. Conclusion

The optimum short-range parameter α_i and the symmetry of the tetragonality of GP(2) zones are calculated by the least squares method from the equi-intensity contour around 2 1 0 reflection of GP(2) zones. This implies that the short-range interaction in the system shows an anisotropy with the f.c.c. symmetry and the GP(2) zone is an ellipsoid, which has the modurated structure characterized by fluctuation of solute concentration. The GP(2) zone is different from the simple layer structure proposed before. The correlation lengths of solute concentration obtained from the diffuse scattering intensity synthesized from the value of α_i are nearly 4.8 nm in length and 10 nm in deameter respectively.

References

[1]   A. Guinier, J. Phys. Radium 3. 129 (1942). , Acta Cryst. 5, 121 (1952).
[2]   V. Gerold, Z. Metallk. 45, 593 & 599 (1954).
[3]   R. Baur, Z. Metallk. 57, 368 (1966).

[4]   R. B. Nicholson and J. Nutting, Phil. Mag. 3, 531 (1958).

[5]   J.R. Parsons, M. Rainvlle and C. W. Hoelke, Phil. Mag. 21, 1105
      (1970).

[6]   V. A. Phillips, Acta Met. 21, 219 (1973).

[7]   H. Yoshida, D. J. Cockayne and M. J. Whelan, Phil. Mag. 34, 89
      (1976).

[8]   C. J. Sparks and B. Borie, Local Atomic Arrangements Studies by
      X-ray Diffraction,Gordon and Breach, New York 1966 (p. 1).

[9]   B. Borie, Acta Cryst. 10, 89 (1957).

[10] M. Hida, M. Yamada and M. Ohta, J. Japan Inst. Metals 40, 888
      (1976).

[11] T. Hirouchi, K. Liu and Y. Murakami, J. Japan Inst. Metals 37,
      1120 (1973).

[12] B. Borie, Acta Cryst. 17, 212 (1964).

[13] S. C. Moss, J. Apple. Phys. 35, 3574 (1964).

[14] J. E. Jr. Gragg and J. B. Cohen, Acta Met. 19, 507 (1971).

[15] H. Terauchi, M. Mori and Y. Yamada, J. Phys. Soc. Japan 32, 1049
      (1972).

[16] J. Frenkel and T. Kontrova, J. Phys. USSR 1, 137 (1939).

[17] B. Horovitz, J. L. Murray and J. A. Krumhansl, Phys. Rev. B18,
      3549 (1978).